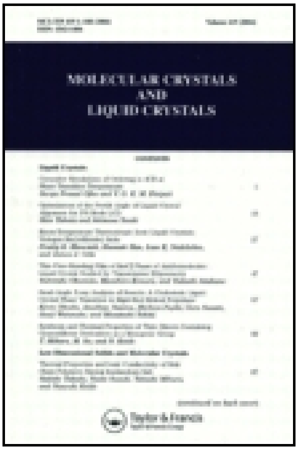

Molecular Crystals and Liquid Crystals
Publication details, including instructions for authors and subscription information:
http://www.tandfonline.com/loi/gmcl16

A New Generation Process and Matrix Representation of Disclinations in Nematic and Cholesteric Liquid Crystals

A. E. Stieb [a b] & M. M. Labes [a]
[a] Department of Chemistry, Temple University, Philadelphia, Pa, 19122
[b] Institut f. Ang. Festkörper-Physik, 7800, Freiburg, W. Germany
Version of record first published: 18 Oct 2010.

Mol. Cryst, Liq. Cryst., 1978, Vol. 45, pp. 21–44

Printed in Holland

A New Generation Process and Matrix Representation of Disclinations in Nematic and Cholesteric Liquid Crystals†

A. E. STIEB‡ and M. M. LABES

Department of Chemistry, Temple University, Philadelphia, Pa. 19122

(*Reeeived January 10, 1977; in final form August 3, 1977*)

Disclinations in nematic liquid crystals are described as transitions between two different states of quantized bulk deformations in a layer. The quantized states of deformation are due to well defined uniform boundary conditions, which allow only discrete solutions of the partial Euler differential equations governing the deformation.

A new continuous generation process for the non-singular disclinations of integer strength is discussed. The local turns of the director field, involved in this process, can be used for an algebraic description of the topological properties of the disclinations. This formalism can also be applied to disclinations of half integer strength and to disclinations in cholesteric liquid crystals. From this theory, the existence of stable disclinations of the strength $s = 0$ can be predicted.

Disclinations of integer strength are created by an experimental process analogous to the new theoretical generation process. Experimental evidence for the existence of disclinations of the strength 0 is given.

1 INTRODUCTION

The elastic free energy G of a nematic liquid crystal for a certain field of the director **N** is

$$G = \frac{1}{2}\int dV(K_{11}(\text{div } \mathbf{N})^2 + K_{22}(\mathbf{N}\cdot\text{curl } \mathbf{N})^2 + K_{33}(\mathbf{N}\times\text{curl } \mathbf{N})^2) \quad (1)$$

where K_{11}, K_{22}, and K_{33} are the Frank elastic constants for splay, twist, and

† This work was supported by the U.S. Army Research Office under contract No. DAHCO4-74-G-0186.

‡ Visiting Research Associate, 1975–1976. Permanent address: Institut f. Ang. Festkörper-Physik, 7800 Freiburg, W. Germany.

bend,[1] and where V is the volume. In an equilibrium state, G is a minimum and the director **N** has to obey the corresponding Euler–Lagrange differential equations. For any specific case, one defines boundary conditions which then allow only certain discrete solutions.

Since a macroscopic nematic layer tends to be uniformly in a discrete ground state, disclinations are unstable except in the case of degeneracy of the states. Experimentally, disclinations originally existing in nematic layers with uniform boundary conditions disappear by shrinking in length and leaving a uniform layer. More or less stable disclinations are only found in layers having nonuniform, weak boundary anchoring. In each case, the known types of disclinations separate areas with different states of bulk alignment.

In this paper we mainly consider disclinations in layers with strong, uniform boundary anchoring. In spite of their instability, they often exist for measurable lifetimes. Their structure has been calculated approximately by neglecting friction effects;[2] also disclination structures in cholesteric liquid crystals have been evaluated.[3] Along a line across the disclination, the director **N** turns through an angle of the order of π over a distance of about a layer thickness. Experimentally, even nonsingular "disclination lines" are observed as microscopic line defects with a limited detectable diameter. At larger distances from the disclination, the deformation state is approximately uniform. Therefore, we can interpret disclinations as transitions between different quantized states of uniform bulk deformations. A set of vectors, which is based on a new theoretical generation process for disclinations, can be found to express the topological properties of a disclination. These vectors can be arranged in an orthogonal matrix describing various types of disclination lines.

2 DISCLINATIONS AS STEPS BETWEEN QUANTIZED BULK DEFORMATIONS

Let us consider the special case in which the director **N** depends only on a Cartesian coordinate z (uniform deformation), and in which the elastic constants for splay and bend are equal (two constant approximation). Then:

$$\frac{\partial \cdots}{\partial x} = 0; \qquad \frac{\partial \cdots}{\partial y} = 0; \qquad K_{11} = K_{33} = K_{22}/k \tag{2}$$

The number k indicates the relative magnitude of the elastic constants for twist and bend. With the usual polar coordinates θ and ϕ, the director field

N can be written as

$$\mathbf{N}(z) = \begin{bmatrix} N_1 \\ N_2 \\ N_3 \end{bmatrix} = \begin{bmatrix} \sin\theta \cdot \cos\phi \\ \sin\theta \cdot \sin\phi \\ \cos\theta \end{bmatrix} \quad (3)$$

where $\theta = \arccos(N_3)$ and $\phi = \mathrm{arctg}(N_2/N_1)$.

The elastic free energy derived from (1) with (2) and (3) is:

$$G = \int \mathrm{d}V \cdot \frac{K_{11}}{2}(\theta_z^2 + \phi_z^2 \cdot \sin^2\theta - (1-k)\phi_z^2 \cdot \sin^4\theta) \quad (4)$$

The suffixes of θ and ϕ indicate the derivative with respect to the given coordinate. In an equilibrium state, the director field should show a minimum of the free elastic energy and θ and ϕ should satisfy the partial Euler–Lagrange differential equations, which are in this case:

$$\theta_{zz} - \phi_z^2 \cdot \sin\theta \cdot \cos\theta \cdot (1 - 2(1-k)\sin^2\theta) = 0$$
$$\theta_{zz}\sin\theta(1 - (1-k)\sin^2\theta) + 2\theta_z\phi_z\cos\theta(1 - 2(1-k)\sin^2\theta) = 0 \quad (5)$$

After introducing boundary conditions, only discrete solutions of the equations (5) exist. This corresponds to most of the applications, where layers with uniform and strong boundary anchoring are used. Let us therefore assume the following boundary conditions at $|z| = d/2$ on the glass plates of a sandwich cell (planar parallel alignment):

$$\phi(-d/2) = 0 \qquad \theta(-d/2) = -\pi/2 \quad (6)$$
$$\phi(+d/2) = r_1\pi \qquad \theta(+d/2) = -\pi/2 + r_2\pi$$

The numbers r_1 and r_2 are integers, and d is the cell thickness. For these boundary conditions, simple solutions of the Eqs. (5) exist, which are uniform in the x–y-plane:

$$\phi_1(z) = r_1\pi/2 + r_1\pi z/d \qquad \theta_1(z) = -\pi/2 \quad (7)$$
$$\phi_2(z) = 0 \qquad \theta_2(z) = (r_2 - 1)\pi/2 + r_2\pi z/d \quad (8)$$

Solution (7) describes a pure twist deformation, and (8) a splay-bend deformation. The quantum numbers r determine the number of π-turns of the director **N** about an axis perpendicular to the boundary alignment direction $\mathbf{N}_0$. Both solutions can be transformed into one another by a uniform turn of **N** about the direction of $\mathbf{N}_0$ through an angle of $|\alpha| = \pi/2$. We will call this director field operation a "bend twist transformation" and consider it as a part of a new generation process of disclinations.

The stability of the deformations (7) and (8) depends on the relative magnitude of the elastic constants. The energy per unit area of the deformations (7) and (8) and of all their intermediate states, characterized by the intermediate turn angle α of the bend twist transformation, is:

$$G/F = (k \cdot \sin^2 \alpha + \cos^2 \alpha)\pi^2 K_{11} r^2/2d \quad (9)$$

F is the area of the liquid crystal layer. The twist deformation ($\alpha = \pm\pi/2$) is stable for $k < 1$ and the splay-bend deformation ($\alpha = 0$) is stable for $k > 1$. In the one constant case ($k = 1$), the deformation is continuously degenerate for all α.

Let us now consider two adjacent deformed areas with the quantum numbers r and $r + 2s$ (s half integer or integer), the transition region between the two areas being a disclination. The change in the number of 2π-turns of the director between these bulk deformations defines the strength s of the disclination. In this way the existence of disclinations is related to the quantized bulk deformations, which result themselves from strong and uniform boundary anchoring. In a similar way as other authors,[4,5] we will speak of "twist disclinations" if $k < 1$, where twist deformations are preferred by the layer to the related splay-bend deformations, and of "wedge disclinations" if $k > 1$.

If there is no strong boundary anchoring, coreless surface disclinations are possible as well as disclinations ending on the glass surfaces with singular points. In the case of Frank disclinations,[1] for example, no restricting boundaries were taken into account, and the energy of a single line is not finite.

3 GENERATION PROCESS FOR DISCLINATIONS OF INTEGER STRENGTH

The Volterra process, applied by Friedel and De Gennes to describe topologically the generation of disclinations, is well suited for disclinations of half-integer strength.[5,6] This hypothetical process is discontinuous, and the structure of the core of the generated disclinations is considered to be singular. However, disclinations of integer strength have been observed to be non-singular,[7,8,2] and the appropriate generation process should be continuous.

In order to create the required bulk deformations, which are associated with the disclinations, we will use the bend twist transformation of a directorfield. This transformation is degenerate, since expression (9) does not depend on the sign of the angle α, and the two possible states have the same energy. Let us start with a planar homogeneous nematic layer, whose director $\mathbf{N}_0$ is constant, and whose boundary anchoring is strong. The generation of the bulk deformation and its limiting disclination can be envisaged as follows:

1) Determine a plane Σ limited by a closed line L in a nematic layer with a homogeneous alignment $\mathbf{N}_0$.

2) Turn the director $\mathbf{N}$ in all points of the plane Σ about an axis $\mathbf{T}$ through an angle of $\tau = t\pi$, where τ decreases rapidly to zero at the edges of Σ, and where $\mathbf{T}$ is perpendicular to $\mathbf{N}_0$ ($t = \pm 1$).

3) Turn $\mathbf{N}$ about $\mathbf{N}_0$ through a constant angle of $\alpha = +n\pi/2$ above Σ, and through $\alpha = -n\pi/2$ below Σ ($n = \pm 1$).

4) Let the director field relax to its state of minimum energy.

The result is a disclination loop of the strength 1 along the line L, enclosing a quantized bulk deformation, which is superimposed on the original director field. We define the quantum number r of the deformed state to be positive if $\mathbf{N}$ on a line along $\mathbf{\Sigma}$ turns anticlockwise for the positive viewing direction. An example of the process is shown schematically in Figure 1 for twist disclinations ($k < 1$) with the parameters $t = +1$ and $n = +1$ of the director turns. The lines, "nails", and points in the figure indicate the direction of the local optical axis $\mathbf{N}$, where the heads of the nails point out of the figure plane. In Fig. 1a, the position of the plane Σ in the middle of the two boundary plates is indicated by a dashed line. $\mathbf{\Sigma}$ is a unit vector, which is perpendicular to the plane. Σ is limited on both sides by the line L, which is closed to a loop at remote points above and below the figure plane. The direction of the left border line is that of the viewing direction and is characterized by a unit vector $\mathbf{L}$. The process is started by turning $\mathbf{N}$ in all points of Σ about a vector $\mathbf{T}$, which is perpendicular to $\mathbf{N}_0$. In this special case, $\mathbf{N}_0$ is parallel to $\mathbf{L} \times \mathbf{\Sigma}$ and $\mathbf{T}$ parallel to $\mathbf{L}$. In Figure 1b, the complete turn about $\mathbf{T}$ with $\tau = +\pi$ is shown. The turn may be characterized by the length and the sign of the vector $\mathbf{T}$, so that $|\mathbf{T}| = |t|$ ($t = \pm 1$ for integer strength disclinations). In what follows below, we will refer to t as the "core parameter".

Over a distance of d at the edges of Σ the angle τ may decrease rapidly to 0. In this state, as shown schematically in Figure 1b, the energy of the director field has a maximum according to (9). Instead of allowing the deformation to relax back to its absolute energy minimum, we apply the bend twist transformation and use its degeneracy mentioned above. The director $\mathbf{N}$ is turned about the direction of $\mathbf{N}_0$ through a constant angle of $\alpha = +n\pi/2$ above Σ, and $\alpha = -n\pi/2$ below Σ. Outside of this volume, limited by a vertical plane through L, the angle τ has to decrease, for example, linearly to 0 in a radial direction from the line L. The turn angle α has then to decrease sectorially from $\pm\pi/2$ in the vertical plane through L to 0 in the horizontal plane through L. There is no physical discontinuity involved, not even in the line L, because there the director $\mathbf{N}$ is parallel to $\mathbf{N}_0$, so that no α-turn has an effect on the alignment in L itself. An intermediate state of this turn is shown in Figure 1c. After completing the transformation, we have

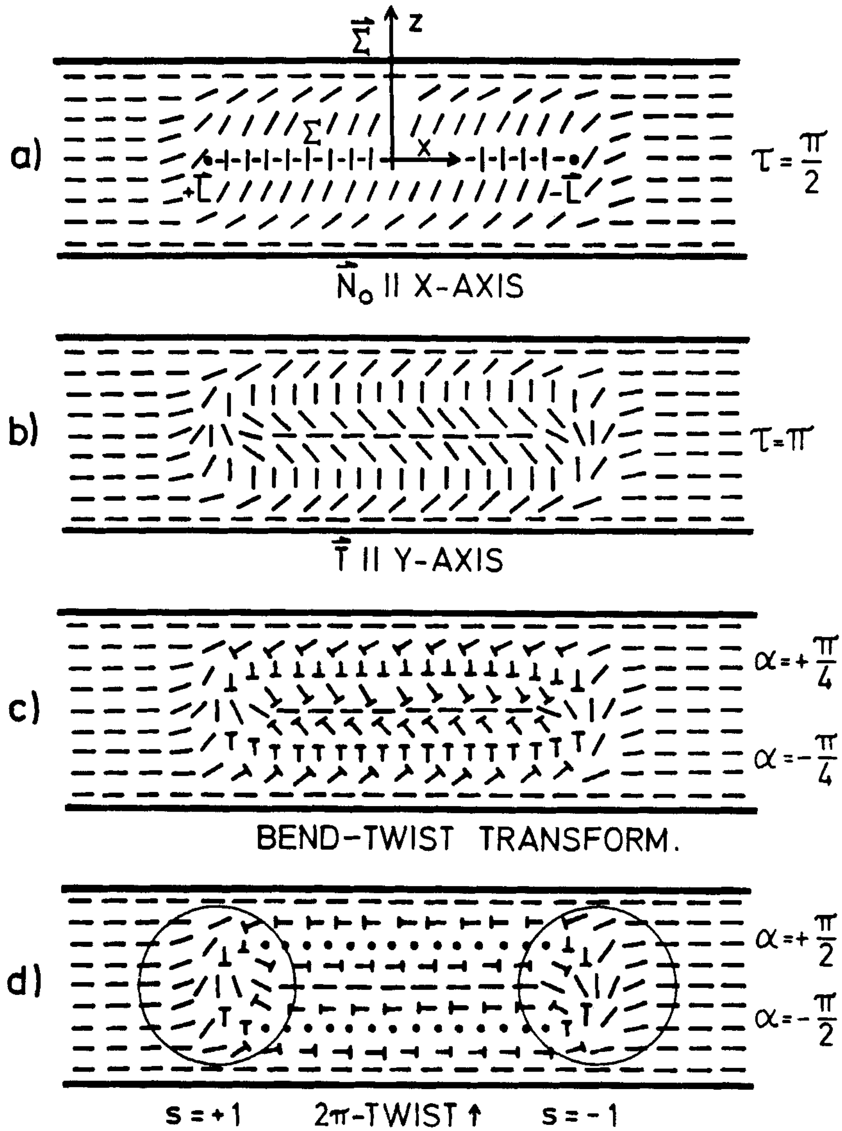

FIGURE 1 Cross sections through the director field in different states of the continuous generation process for a pain of integer strength disclinations: a) position of the plane Σ (dashed line) between the boundary plates and local rotation of **N** in Σ about **T** through an angle of $\tau = +\pi/2$; b) rotation of **N** about **T** through $+\pi$; c) turn of **N** about $\mathbf{N}_0$ through $|\alpha| = \pi/2$ in opposite senses above and below Σ (bend twist transformations); d) final uniform twist deformation separated from the undeformed parts on both sides by twist disclinations of the strength $s = \pm 1$ (encircled) which are closed to a loop outside the figure plane.

a uniform twist deformation with a twist axis perpendicular to the boundary plates (see Figure 1d). In this state, the elastic free energy has a relative minimum with $G/F = 2\pi^2 k K_{11}/d$, so that this state is metastable. The overall twist angle ρ between the boundary plates is

$$\rho = r\pi = 2nt\pi \tag{10}$$

while outside the loop no deformation is generated. Generally, the deformation state of a homogeneous layer after completing the generation process can be characterized by a vector

$$\mathbf{R} = n[\mathbf{N}_0 \times \mathbf{T}] \qquad \text{with} \quad |\mathbf{R}| = r \tag{11}$$

since on a line drawn perpendicularly through the layer, the direction of the nematic axis turns about this vector $\mathbf{R}$ through $r\pi$. The transition between the original state $\mathbf{R}_1$ and the new state $\mathbf{R}_2$ with the corresponding quantum numbers r_1 and r_2 is formed by the disclination loop whose strength we define to be

$$s = (r_2 - r_1)/2 = n \cdot t \tag{12}$$

This definition is identical with that of Nehring[2] and equivalent to the Frank[1] definition. The two encircled disclinations in Figure 1d, limiting the twist deformation on both sides, have according to (12) opposite signs of s and t. The line L has changed direction by 180 degrees from $+\mathbf{L}$ to $-\mathbf{L}$, and from left to right the twist deformation in Figure 1d is increasing at $+\mathbf{L}$ and decreasing at $-\mathbf{L}$.

The stability of the disclinations depends on the stability of their generative bulk deformations, and therefore on the relative magnitude of the elastic constants $k = K_{22}/K_{11}$. In the case of $k > 1$ (not observed in experiment), expression (9) has a minimum when $\alpha = 0$, and wedge disclinations are stable. For $k < 1$ twist disclinations are stable. In nematic liquid crystals, one often finds that $k \sim 1/2$.

Examples of cross sections through bulk deformations limited on both sides by disclinations of opposite sign are given in Figure 2a and b for different directions of the line L with respect to $\mathbf{N}_0$. All intermediate forms are possible and change continuously along the closed disclination loop. The model of Fig. 2a and b is confirmed experimentally by the observation that the disclination appears in the extraordinary ray of light as a cylindrical diffraction lense, irrespective of the direction of the disclination in the layer. In Figure 2c, the corresponding pattern for a layer with homeotropic boundary alignment is shown. If the process is to be applied to a layer which is already in a deformed state, it has to be carried out in a sufficient thin layer about the plane Σ, where the alignment has to be (nearly) uniform. The plane Σ can also be replaced by a limited surface of any shape which even may be continued in an

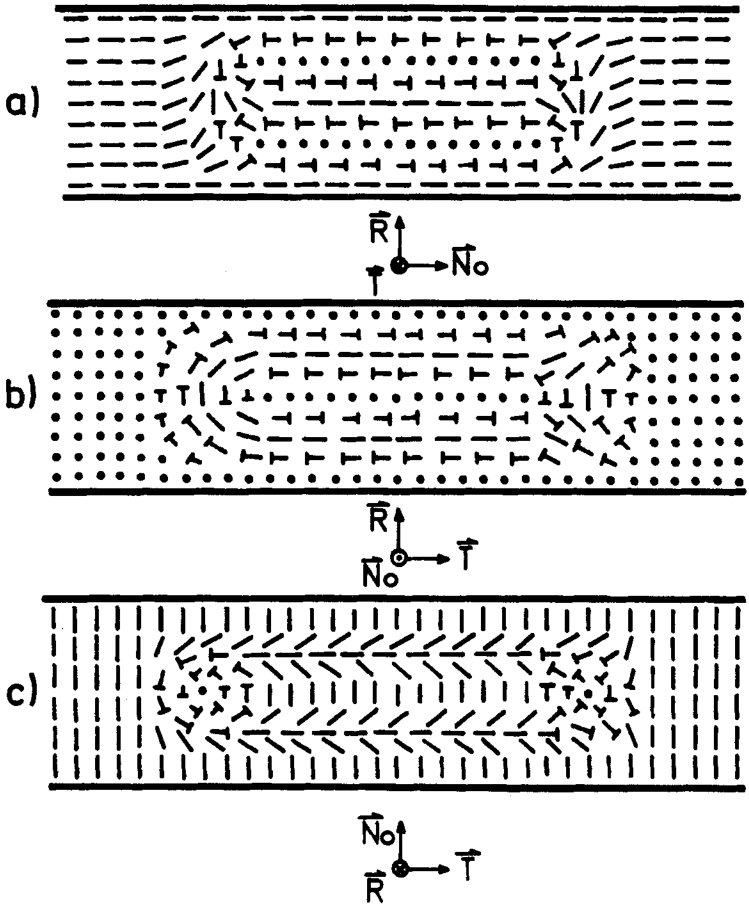

FIGURE 2 Cross sections through small loops of twist disclinations of integer strength, enclosing areas of uniform bulk deformation. The directions of the vectors N_0, T and **R** are indicated below each figure. The related wedge disclinations can be constructed from these patterns by the twist bend transformation (turn N through $\pi/2$ about N_0).

imaginary directorfield outside the actual layer. The process can be modified for the generation of half integer disclinations by using a turn angle of $|\tau| = \pi/2$ about T and by introducing a cut surface in the plane Σ. In this case, the result is the same as that of the de Gennes process.[5,6]

Disclinations of integer strength have no line singularities as do half-strength disclinations, but they can have an even number of singular points. These singular points cannot be generated by the continuous process outlined above. One has to introduce a discontinuity plane across the loop of L, which cuts the directorfield into two parts during the generation process. The process is then performed independently in those two regions with opposite signs of the turn angles τ and α. By this, two identical bulk deformations are received. They can again be connected without discontinuity, except at the intersections of the line L with the discontinuity plane, where singular points remain. At the singular points, only the sign of the core parameter is changed, but not the strength of the disclinations.

4 ALGEBRAIC DESCRIPTION OF THE TOPOLOGICAL PROPERTIES OF THE DISCLINATIONS

The generation process outlined above defines only the topological properties of disclinations, which mainly involve the turn differences in the adjoining deformations and the turn of the director along a line across the center of the disclination. The actual structures of the disclinations are slightly different from those shown schematically in Figure 2 and depend, for example, on the relative magnitude of the elastic constants.

In the conception of disclinations as steps between different quantized bulk deformations we do not have to make a principal distinction between integer and half integer steps. We can, therefore, also include in our considerations disclinations of half integer strength as well as "disclinations of zero strength" which will be defined below. Let us use the following vectors to characterize a disclination, after defining the plane Σ between the boundary plates and the direction $\mathbf{L}$ of the disclination line:

1) The unperturbed director $\mathbf{N}_0$ about which the second turn in the generation process is carried out;

2) The axis $\mathbf{T}$ about which the first turn in the generation process is carried out and which is perpendicular to $\mathbf{N}_0$;

3) The vector $n(\mathbf{N}_0 \times \mathbf{T}) = (\mathbf{R}_2 - \mathbf{R}_1) = \Delta\mathbf{R}$, which describes the difference of the deformation states on both sides of the disclination (comparable to a Burger's vector).

It is convenient to arrange these three vectors as columns of an orthogonal "disclination matrix"

$$\bar{D} = [\mathbf{N}_0, \mathbf{T}, n(\mathbf{N}_0 \times \mathbf{T})] \tag{13}$$

The redundant information of this matrix will be useful in the case of the zero strength disclinations.

In Table I, the disclination matrices $\bar{D}$ of the disclinations shown in Figure

TABLE I

Matrix representation of the integer strength disclination lines shown in Figure 2 with the enclosed deformation states **R**. The Cartesian coordinate system is fixed with its x-, y-, and z-axes to the directions of the vectors $\mathbf{L} \times \mathbf{\Sigma}$, $\mathbf{L}$, and $\mathbf{\Sigma}$. The columns of the matrices represent the vectors $\mathbf{N}_0$ (unperturbed nematic axis and second turn axis in the generation process), $\mathbf{T}$ (first turn axis), and $\Delta\mathbf{R} = n(\mathbf{N}_0 \times \mathbf{T})$ (difference of the deformation states).

$\begin{bmatrix} 1 & 0 & 0 \\ 0 & 1 & 0 \\ 0 & 0 & 1 \end{bmatrix}$	$\begin{bmatrix} 0 \\ 0 \\ 1 \end{bmatrix}$	$\begin{bmatrix} 1 & 0 & 0 \\ 0 & -1 & 0 \\ 0 & 0 & -1 \end{bmatrix}$
$\begin{bmatrix} 0 & 1 & 0 \\ -1 & 0 & 0 \\ 0 & 0 & 1 \end{bmatrix}$	$\begin{bmatrix} 0 \\ 0 \\ 1 \end{bmatrix}$	$\begin{bmatrix} 0 & -1 & 0 \\ -1 & 0 & 0 \\ 0 & 0 & -1 \end{bmatrix}$
$\begin{bmatrix} 0 & 1 & 0 \\ 0 & 0 & 1 \\ 1 & 0 & 0 \end{bmatrix}$	$\begin{bmatrix} 0 \\ 1 \\ 0 \end{bmatrix}$	$\begin{bmatrix} 0 & -1 & 0 \\ 0 & 0 & -1 \\ 1 & 0 & 0 \end{bmatrix}$

2 are listed following the same sequence as employed in the figure. A disclination matrix transforms the state $\mathbf{R}_1$ into the state $\mathbf{R}_2$ according to

$$\mathbf{R}_2 = \mathbf{R}_1 + \bar{D} \cdot \mathbf{E}_3, \qquad \text{where} \quad \mathbf{E}_3 = \begin{bmatrix} 0 \\ 0 \\ 1 \end{bmatrix} \tag{14}$$

The disclination matrices for an arbitrary direction of $\mathbf{N}_0$ with respect to the line direction $\mathbf{L}$ can easily be derived from the matrices given in Table I by a space transformation. Together with the director $\mathbf{N}_0$, the disclination matrix $\bar{D}$ has to be rotated about the appropriate axis:

$$\bar{D}_2 = \bar{B} \cdot \bar{D}_1 \tag{15}$$

$\bar{B}$ is an orthonormal rotation operator whose form, for example, for a rotation about the z-axis through an angle of β is

$$\bar{B} = \begin{bmatrix} \cos\beta & -\sin\beta & 0 \\ \sin\beta & \cos\beta & 0 \\ 0 & 0 & 1 \end{bmatrix}$$

Applying this operation with $\beta = \pi$ to the left disclination in Figure 2a, we receive the right disclination in Figure 2a seen from the backside of the figure. In order to avoid complications, we will consider only parallel disclinations seen in the same direction, using the matrices given in Table I.

If there is a singular point on the disclination line, then the change of the $\bar{D}$-matrix at this point is carried out by the operation

$$\bar{D}_2 = \bar{D}_1 \cdot \bar{P} \tag{16}$$

with

$$\bar{P} = \begin{bmatrix} 1 & 0 & 0 \\ 0 & -1 & 0 \\ 0 & 0 & 1 \end{bmatrix}$$

The operator $\bar{P}$ changes only the sign of the core parameter t and not that of the strength s. On a closed loop of an integer strength disclination only an even number of singular points is found.

The matrix notation can also be applied to disclinations of half integer strength. The parameters t and s then have half of the absolute values of the parameters characterizing integer strength lines. An example of a matrix for a half integer line, where a left handed turn increases by π and where $\mathbf{N}_0$ is parallel to the line direction, is

$$\bar{D} = \begin{bmatrix} 0 & \pm\frac{1}{2} & 0 \\ 1 & 0 & 0 \\ 0 & 0 & \frac{1}{2} \end{bmatrix} \tag{17}$$

As the core structure of the half integer disclinations is not known exactly, the sign of t is left arbitrary; the direction of $\mathbf{T}$ is defined to be perpendicular to $\Delta\mathbf{R}$ and $\mathbf{N}_0$.

5 INTERACTION OF DISCLINATIONS

The law, that disclinations with opposite signs of s attract themselves while disclinations with the same signs repel,[9] is not generally true. Consider, for example a pair of integer strength disclinations in a layer with planar boundary conditions and with $\mathbf{L} \perp \mathbf{N}_0$. The state $\mathbf{R}_1$ outside the two disclinations and the state $\mathbf{R}_2$ between them may be

$$\mathbf{R}_1 = \begin{bmatrix} 0 \\ 0 \\ r \end{bmatrix} \qquad \mathbf{R}_2 = \begin{bmatrix} 0 \\ 0 \\ r + r' \end{bmatrix}$$

where r is positive. The strengths of the two disclinations $\bar{D}_1$ and $\bar{D}_2$ are then of different signs irrespective of the sign of r'. In a nematic layer, the two disclinations approach one another if r' is positive and migrate away from each other if r' is negative. This is a consequence of the fact that deformation states of lower free elastic energy are more stable than states with higher free energy. The attraction law of disclinations can be replaced by the following simple rule:

Parallel disclinations, separating regions of different deformation states in a nematic layer, move in such a way that regions with lower free elastic energy expand at the expense of higher states.

Some examples for positive r are given in Figure 3. The disclinations move in the direction indicated by the arrows. For $r < 0$ all the arrows in Figure 3 have to be reversed; in the case of $r = 0$, the disclinations of a pair migrate away from each other.

The splitting and merging of parallel disclinations can be expressed in the matrix notation by

$$\bar{D}_3 = \bar{D}_1 + \bar{D}_2 - [\mathbf{N}_0, \mathbf{0}, \mathbf{0}] \tag{18}$$

The last term in (18) ensures that the first column of the matrix is constant. Let us now examine several cases:

a) Combination of two disclinations of half integer strength leads either to an annihilation or to a disclination of integer strength. We have to use

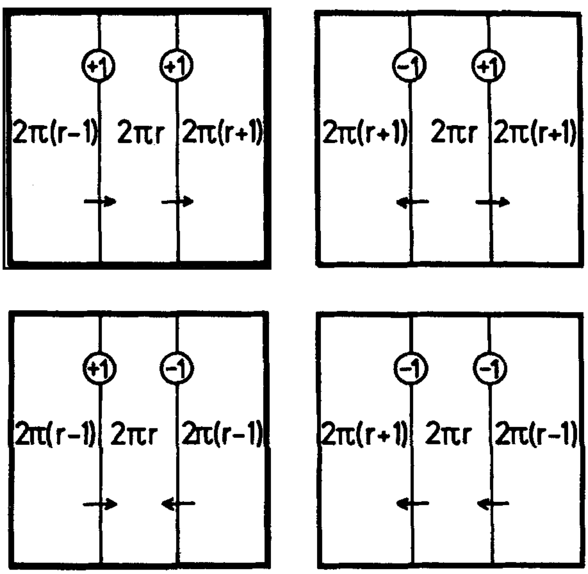

FIGURE 3 Motion of disclination lines of integer strength in a nematic layer. The disclinations separate areas of different deformation states, indicated by the different turn angles of the director (multiples of π). The strength of the disclination lines is shown in the circles, and the direction of migration for positive r is given by the arrows.

only the positive or only the negative signs of t for both of the two lines, but it cannot be determined which set of both is to be used, since in experiment the two modes of the core in the resulting integer strength disclination can occur with equal probability.

b) Addition of integer strength disclinations with the same sign of s does not occur, according to the law demonstrated in Fig. 3. No stable disclinations of the strength $s = 2$ have been found experimentally.

c) The merging of attracting integer strength lines results in an annihilation, if the signs of the core parameters are different. For equal values of t, a new kind of disclination of the strength 0 is formed (see Figure 4).

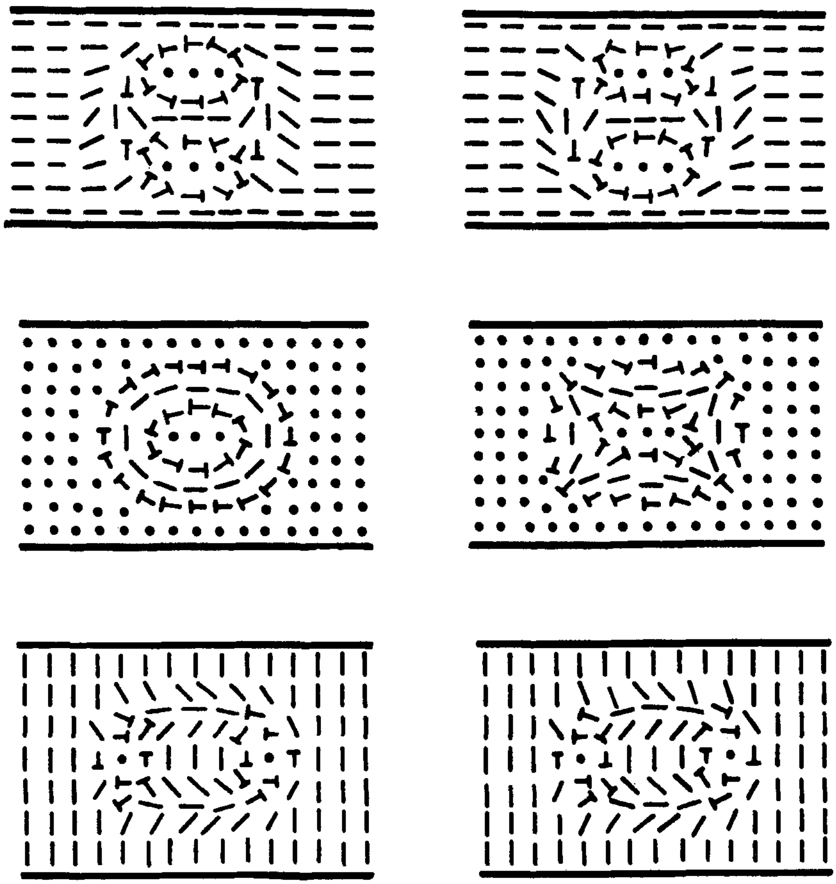

FIGURE 4 Disclinations of the strength zero for different orientations of the line direction with respect to the unperturbed director N_0 (twist type disclinations; corresponding wedge type by the twist bend transformation).

This special case can be envisaged by reversing the core of the disclination on the right side of Figure 2b by operation (16). Both disclinations will approach and merge, but they cannot annihilate. According to (18), the pair forms a new type of disclination with the parameters $s = 0$ and $|t| = 2$:

$$\bar{D}_3 = \begin{bmatrix} 0 & 1 & 0 \\ -1 & 0 & 0 \\ 0 & 0 & 1 \end{bmatrix} + \begin{bmatrix} 0 & 1 & 0 \\ 0 & 0 & 0 \\ 0 & 0 & -1 \end{bmatrix} = \begin{bmatrix} 0 & 2 & 0 \\ -1 & 0 & 0 \\ 0 & 0 & 0 \end{bmatrix}$$

The structure of the resulting disclination is shown in Figure 4 (left central pattern), together with several other examples. The patterns resemble, in part, those of the Frank disclinations of integer strength[1]. The main difference between the two disclination types is due to the core structure and the boundary conditions. The matrices of the disclinations shown in Figure 4 are listed in the same sequence in Table II. Further disclinations of the strength zero can be obtained from the given examples by the twist bend transformation. They are of the wedge type and only stable for $k > 1$.

A generation process for the zero strength disclinations consists of a two-fold application of the generation process described above. After generating the first loop, a second loop inside the first one is generated by using the same turn axes in reversed sequence. This annihilates the first bulk deformation inside the second loop. The two lines approach and merge, and only a residue of the bulk deformation is left in the center of the disclination. The axis of this residual director turn is needed for the complete characterization of the disclination. Using the appropriate positive or negative direction of $\mathbf{N}_0$ in the D-matrix, the residual director turn is given by the vector product $\mathbf{N}_0 \times \mathbf{T}$.

TABLE II

Matrix representation of the disclinations of the strength zero shown in Figure 4 (same sequence).

$\begin{bmatrix} 1 & 0 & 0 \\ 0 & 2 & 0 \\ 0 & 0 & +0 \end{bmatrix}$	$\begin{bmatrix} 1 & 0 & 0 \\ 0 & -2 & 0 \\ 0 & 0 & -0 \end{bmatrix}$
$\begin{bmatrix} 0 & 2 & 0 \\ -1 & 0 & 0 \\ 0 & 0 & +0 \end{bmatrix}$	$\begin{bmatrix} 0 & -2 & 0 \\ -1 & 0 & 0 \\ 0 & 0 & -0 \end{bmatrix}$
$\begin{bmatrix} 0 & 2 & 0 \\ 0 & 0 & +0 \\ 1 & 0 & 0 \end{bmatrix}$	$\begin{bmatrix} 0 & -2 & 0 \\ 0 & 0 & -0 \\ 1 & 0 & 0 \end{bmatrix}$

Let us summarize the most important properties of the zero strength disclinations to be expected in an experiment. On both sides of the disclination, the states of the bulk deformations should be the same. The disclinations should have some similarity with pairs of disclinations or a double line character. Their thickness should be approximately the layer thickness. They must not be closed loops, since the bulk deformation states on both sides are the same. In this case, a pair of singular points would be required at the two ends of the zero strength disclination line.

6 DISCLINATIONS IN CHOLESTERIC LIQUID CRYSTALS

Defect lines in cholesteric liquid crystals have been explained in terms of λ, τ, and χ disclinations.[10] The lines parallel to the cholesteric planes have been referred to as λ and τ disclinations, while the half integer disclination lines in Cano wedges[11] with a planar boundary alignment have been interpreted as χ-disclinations.[4,12] In most of the theoretical considerations, the boundary conditions have not been taken into account properly, and no consistent definition of the strength of these disclinations has been worked out. Several effects predicted from theory have not been observed, as, for example, the splitting of half integer strength lines into a couple of singular lines,[12] or the straight line property of the λ and τ disclinations.[10,13] The proposed core structures[10] and singularity rules[13,14] seem partly to be wrong.

Other authors, for example Saupe[15] and Nehring,[2] have stated that the disclinations in nematics and in cholesterics should be very similar as a consequence of the close similarity of the nematic and cholesteric phases. The calculations of Nehring[2] and Scheffer[3] show the similarity of the disclinations in planar twisted layers of nematics and in cholesterics. We cannot see any basic topological difference between a twisted nematic and a cholesteric liquid crystal of large pitch, and therefore apply the new generation process and matrix formalism to cholesteric liquid crystals.

Consider a Grandjean–Cano wedge,[11] where the boundary alignment is parallel to the x-direction. The layer is twisted about the z-axis through different multiples r of the angle π. The director in the center of the layer is either parallel to the x-axis or to the y-axis, depending on the even or uneven number r. The disclinations, as steps between areas of different turn numbers r, can be generated in a thin sheet of the layer in the same way as shown in Figure 1. They can be described by disclination matrices of the form:

$$\bar{D} = \begin{bmatrix} \cos\delta & t\cdot\sin\delta & 0 \\ -\sin\delta & t\cdot\cos\delta & 0 \\ 0 & 0 & s \end{bmatrix} \quad \text{where} \quad \delta = \pi(r/2 + s) \qquad (19)$$

The strength s and the core parameter t can be integers or half integers.

An example of such a disclination of integer strength is given in Fig. 5b and corresponds to the nematic structure shown in Figure 2a. We propose to replace the double singular $\tau^- - \tau^+$ disclination pairs,[10] whose existence to the knowledge of the authors has not been proved experimentally, by this nonsingular disclination structure (see Figure 5). Similarly, $\lambda^- - \lambda^+$ pairs can be replaced by the pattern given in Figure 2b.

Let us now assume that a disclination line has a direction perpendicular to the cholesteric planes of equal alignment. The twist axis of the undisturbed

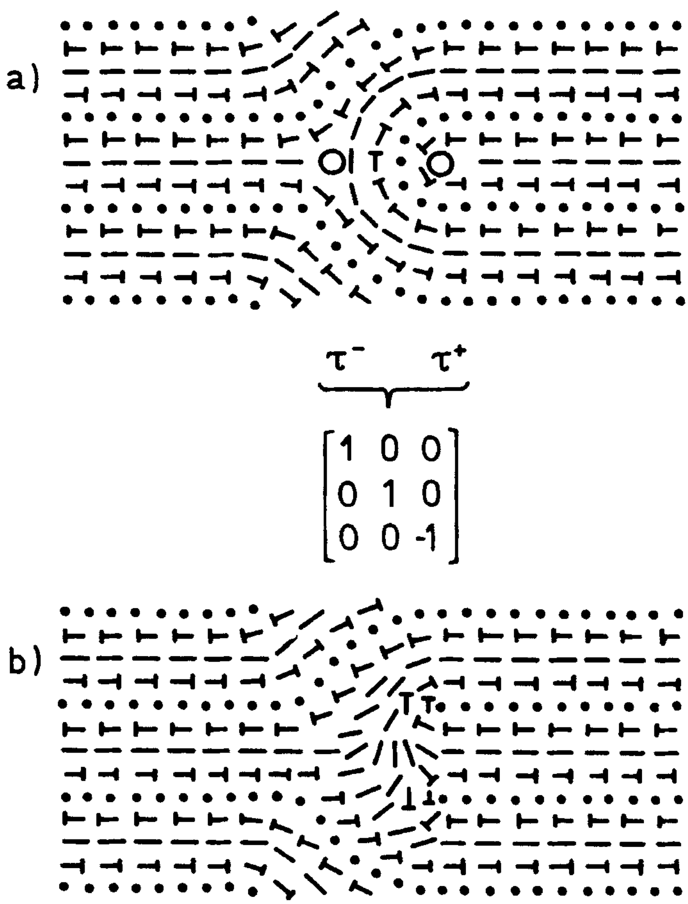

FIGURE 5 Disclinations by insertions of additional twisted layers in a cholesteric liquid crystal. a) $\tau^- - \tau^+$-pair with two singular lines perpendicular to the figure plane (the circles enclose the singular structures); b) replacement of the $\tau^- - \tau^+$-pair by a usual nonsingular disclination of the strength $|s| = 1$.

cholesteric liquid crystal may be parallel to the y-axis, and the alignment in a plane through the coordinate origin parallel to the x-axis. Proceeding along the positive y-axis, the director may turn anticlockwise. We introduce a plane Σ with $z = 0$ whose left border line is given by $x = 0$. In order to generate an integer strength disclination in a similar way as in nematic liquid crystals, we turn the director in all points of the plane Σ about an axis perpendicular to the cholesteric alignment $\mathbf{N}_{0c}$ in the plane Σ. This implies that the vector **T** has to rotate with the cholesteric alignment. After carrying out the T-turn, the two opposite α-turns about the undisturbed cholesteric alignment direction $\mathbf{N}_{0c}$ are applied locally in the same way as in a nematic liquid crystal. The states after the rotations about **T** and $\mathbf{N}_{0c}$ are shown in Figure 6 for a sequence of cross sections through a cholesteric structure, which is repeated periodically. The structure of the disclination is continuous and the vector $\mathbf{N}_{0c} \times \mathbf{T}$ is constant and parallel to the z-axis.

To find the D-matrix of this disclination, we have only to apply the transformation (15) to the appropriate nematic D-matrix. In a cholesteric liquid crystal, this transformation depends on the coordinates. At the origin we have, according to the upper left pattern in Figure 6, the local matrix

$$\bar{D}(z = 0) = \begin{bmatrix} 1 & 0 & 0 \\ 0 & 0 & 1 \\ 0 & 1 & 0 \end{bmatrix}$$

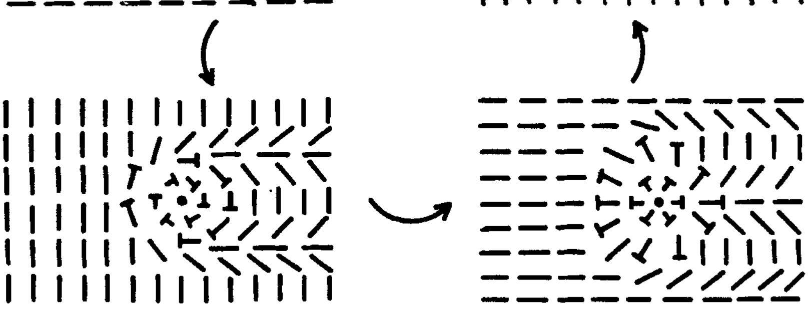

FIGURE 6 Consecutive cross sections through a cholesteric liquid crystal with a disclination line perpendicular to the figure planes.

The turn angle β of the transformation (15) about the y-axis is

$$\beta = 2\pi z/p \qquad p = \text{pitch}$$

The D-matrix of the disclination given in Figure 6 is then

$$\bar{D} = \begin{bmatrix} \cos(2\pi z/p) & -\sin(2\pi z/p) & 0 \\ 0 & 0 & 1 \\ \sin(2\pi z/p) & \cos(2\pi z/p) & 0 \end{bmatrix} \tag{20}$$

There is still another possibility to construct a disclination line with a direction perpendicular to the cholesteric director $\mathbf{N}_{0c}$. The vector $\mathbf{T}$ can be fixed in space, so that the vector $\mathbf{N}_{0c} \times \mathbf{T}$ rotates about the twist axis of the undisturbed cholesteric layer. The matrix of this disclination is:

$$\bar{D} = \begin{bmatrix} \cos(2\pi z/p) & 0 & -\sin(2\pi z/p) \\ 0 & 1 & 0 \\ \sin(2\pi z/p) & 0 & \cos(2\pi z/p) \end{bmatrix} \tag{21}$$

In the bulk deformation related to this disclination, a twist opposite to the spontaneous cholesteric structure is periodically superimposed. This is energetically unfavorable, and may lead to a somewhat different form of the disclination. Depending on the relative size of the elastic constants, the disclination might change its character partly between (20) and (21) and be deformed helicoidally with the period of the cholesteric alignment. Such periodic deformations of disclination lines in cholesteric liquid crystals have been observed, for example, by Rault.[16]

7 COMPARISON WITH EXPERIMENT

Experiments analogous to the continuous generation process have already been carried out in layers with planar boundary alignment.[17,18] A frequency switching technique[19] was used to apply different torques to a layer of a nematic liquid crystal (*WI* from Merck[20]), which shows a change in the sign of its dielectric anisotropy as a function of frequency.[21]

In such an experiment,[17] starting with a homogeneous planar layer, at first a Fréedericksz deformation was carried out by applying a voltage in the frequency regime where the dielectric constant of the liquid crystal is positive. Opposite Fréedericksz deformations are then separated by alignment inversion walls.[22,23,17] In this state, the voltage is switched off during a fraction of a second, in which time the layer begins to realign, while the director in the center of the layer performs a countermovement due to a viscous coupling effect.[24] This is shown schematically in Figure 7. The effect

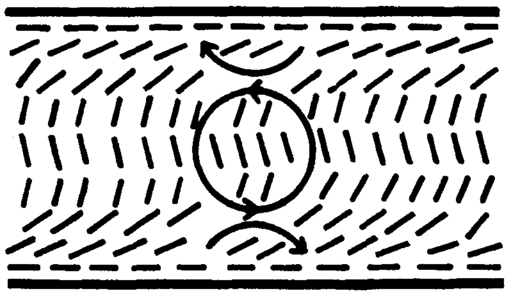

FIGURE 7 Backflow effect in a deformed layer during the realignment by elastic forces. The director in the center of the layer tilts over against the turn direction of the final alignment.

is observed as a consecutive backward and forward movement of the (deformed) conoscopic cross.[17] While the cross is tipping over, a voltage above a certain threshold and of a frequency in the negative dielectric regime is applied. In the center of the layer, the field forces the director into a planar position, and a twist deformation is the result. This twist is of the opposite sense on both sides of the former alignment inversion wall. As a result, the different areas of the layer are twisted by multiples of 2π, and are separated from one another by disclinations of integer strength. The same experiment, then quite analogous to the theoretical process, can be carried out in a layer without alignment inversion walls. Such experiments,[18] for example, have been achieved in a twist cell,[25] and twist deformations with the quantum numbers $r = \pm\frac{1}{2}, \pm\frac{3}{2}, \pm\frac{5}{2}$ have been observed after several frequency switches. Again, the areas of different deformation states were separated by disclination lines of integer strength.

In this work, a cell with planar boundary anchoring and a small overlap area of the electrodes was used. In Figure 8a, a voltage in the frequency regime of positive dielectric anisotropy is applied in this electrode area and a Fréedericksz deformation occurs. After switching the frequency to the negative dielectric regime, the electrode area shows twist deformations with twist angles of $+2\pi$ and -2π (dark and bright areas in Figure 8b). The outer undeformed part of the layer is separated from the twisted areas by an integer strength disclination line. The lines separating the two different twist areas must be disclinations of the strength $s = 2$, because the change of the turn angle is 4π. These lines are extremely unstable, as expected from theory. They split immediately into two disclinations of integer strength with the same sign of s (see Figure 8c). Between the two separated lines, an untwisted area is rapidly expanding in accord with the rules demonstrated in Figure 3.

Disclinations of zero strength have been observed before, but their structure has not been evaluated. Nehring, in the IVth Int. Liquid Crystal Conference, presented a type of defects with the properties, required for zero

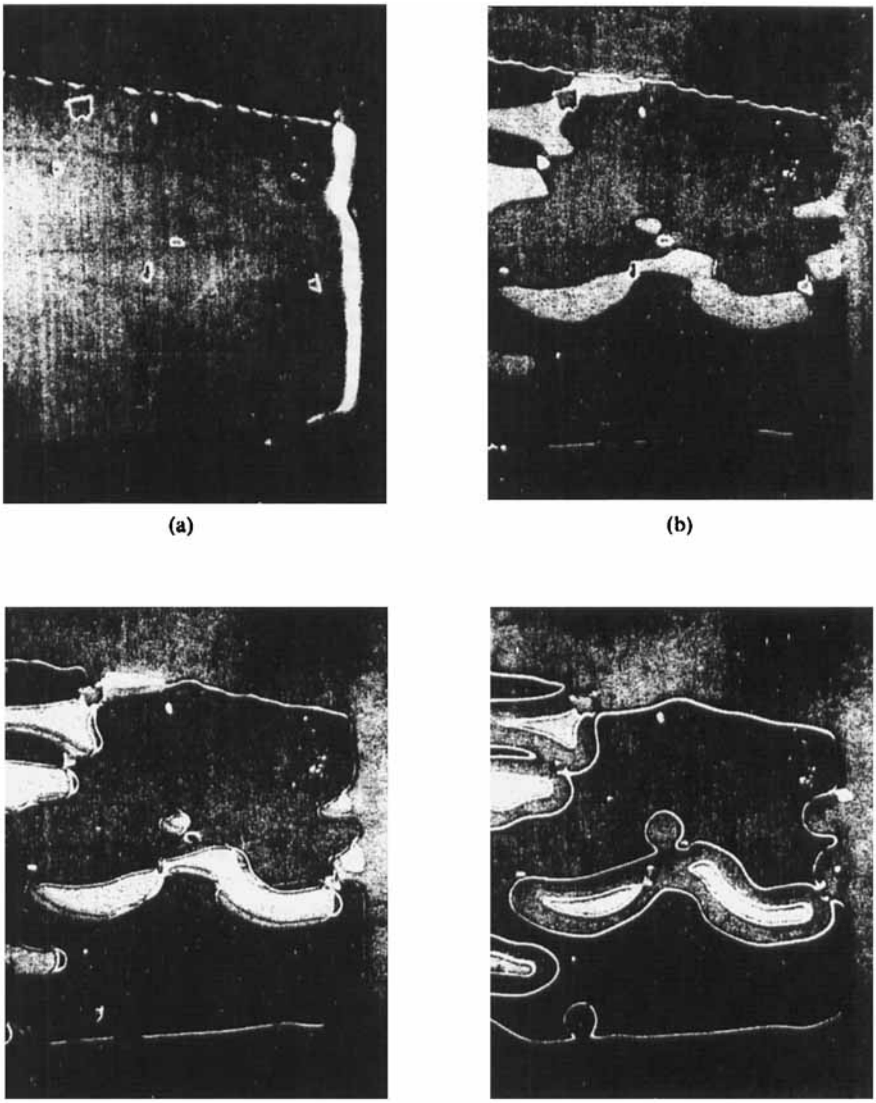

(a) (b) (c) (d)

FIGURE 8 Generation of planar twisted areas and integer strength disclinations, using a liquid crystal with frequency dependent dielectric anisotropy: a) Fréedericksz deformation of the planar layer in the electrode area; b) areas with planar twists of $+2\pi$ and -2π, separated by unstable disclinations of the strength $|s| = 2$ after the frequency switch: c) and d) splitting of the double strength line into a pair of lines of the strengths $|s| = 1$ which move rapidly to increase the width of the untwisted stripe between them (*WI* from Merck; 51 μm; 25 Volts; 3 and 30 kHz; crossed polarizers; magnification 50 times).

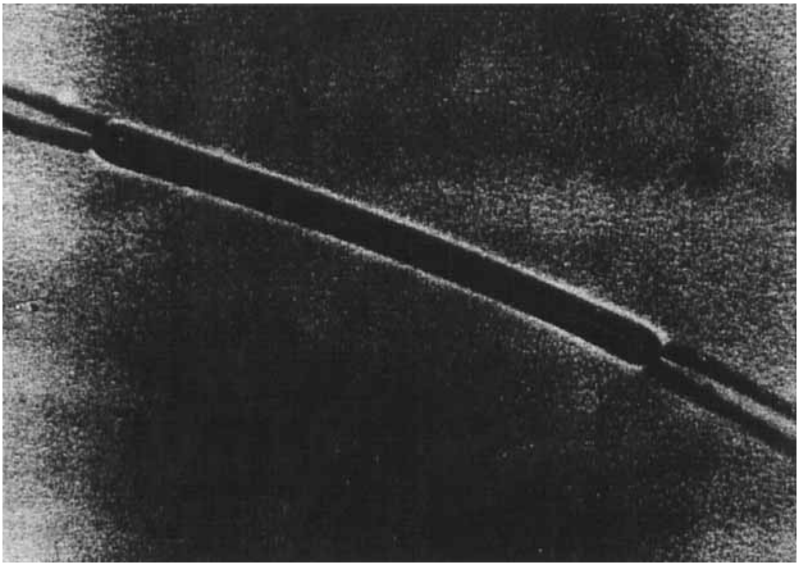

FIGURE 9 Disclination line of the strength 0. Just after switching off the electric field, the Fréedericksz deformation and the S-walls have nearly disappeared while the T-wall has left behind the disclination (planar boundary alignment).

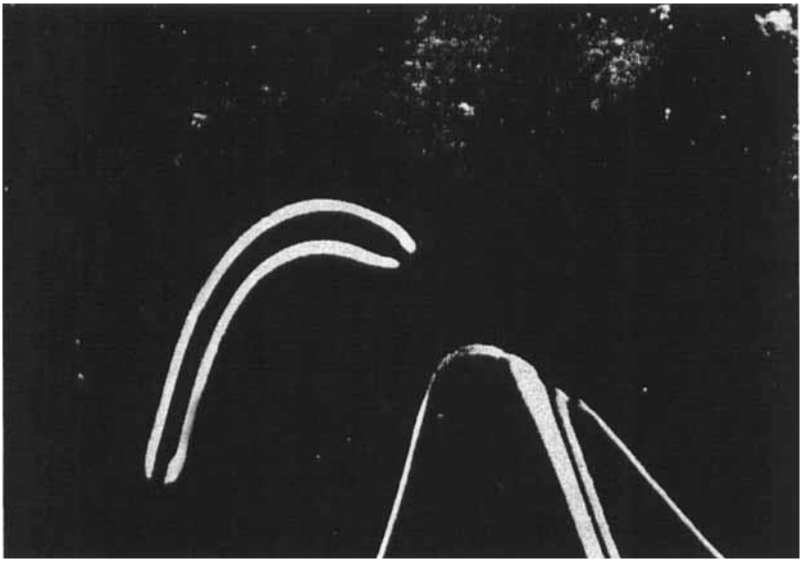

FIGURE 10 Coexisting disclinations of the strength 0, $\frac{1}{2}$, and 1 in a planar layer. The zero strength line ends with singular points; the area enclosed by the sharp half integer line contains π-twists of opposite twist sense. The two opposite twist areas are separated by the integer strength disclination.

strength lines. Another unidentified defect was published on a photograph of the Orsay group.[26] The defect in their Figure 1 has a direction perpendicular to the other disclinations in a Grandjean-Cano wedge. Its total strength must be zero, since the twist deformation on both sides is the same, but its character is different from the zero strength lines. We interpret the defect as a pair of integer strength lines with a vertical distance of one pitch.

Zero strength disclinations are obtained experimentally from alignment inversion walls of the T-type[17,23] by switching off the field, which originally was deforming a layer with a twist of 2π. In Figure 9, the transition of a T-wall into a disclination of zero strength is shown. The S-walls, originally continuing the T-wall at the singular points, are just disappearing after switching off the field. In Figure 10, the coexistence of disclinations of various strengths in a layer with planar boundary anchoring is shown. The area enclosed by the sharp disclination of half integer strength contains twists of $+\pi$ and $-\pi$ and a disclination of the strength 1. The disclination of the strength 0 is to be seen in an untwisted area. It is shrinking in length, and finally the two singularities at its ends merge and annihilate. All the effects shown here are in agreement with the considerations given above.

8 DISCUSSION

It is important to emphasize the necessity for well defined boundary conditions in both experiment as well as theory of disclinations. Soft or nonuniform boundary anchoring complicates the structure of defects considerably and can make it impossible to identify them, especially in cholesteric liquid crystals. Surface disclinations can only exist if the surface anchoring is sufficiently weak. In this case, the core of singular disclination lines can even be eliminated.[27] If the director field is continued beyond the border plates of the layer, an imaginary core must be found outside the layer in the case of half integer disclination lines. Disclinations can even end on the glass surfaces, as is often observed in the "Schlieren-texture." Here, the bulk deformations are to be thought of as continuing and the disclinations closing to loops outside the layer. The vertical disclinations in "Schlieren-textures" are similar to lines of the "Frank-type."

Ericksen[28] pointed out that a single disclination of the Frank type (with relaxed core[7,8] and vertical direction to the boundary plates) might not exist because of its infinite elastic energy. He proposed taking into account pairs or even numbered groups of disclinations whose energy would be finite because of compensation effects at long distances from the couples. In our picture, two Frank disclinations as cut-off parts of one disclination loop are linked by their common bulk deformation, so that only an even number of disclinations can exist.

Nabarro considered disclinations in layers between parallel boundary plates in another way.[29] He interpreted the bulk deformations as alignment inversion walls, which are confined to the space between the plates. In analogy to magnetic structures, the disclinations are then Bloch and Néel lines, separating those parts of the Néel and Bloch walls which have an opposite turn sense. In this interpretation, the singular points separate such parts of the Bloch and Néel lines, which have opposite core structures.

Let us now discuss in more detail the λ and τ structures proposed by Kleman and Friedel[10] for disclinations in cholesteric liquid crystals. In their figures, the authors do not specify any boundary conditions and leave voids in the liquid crystal specimens. In practice one is usually concerned with flat sandwich cells, and we will therefore assume planar boundary conditions. Consequently, we have to fill the voids and fold together the cholesteric layers. This leads to structures called by the authors "pairs of disclinations". But no real pairs, showing two parallel, closely neighboured singular lines, have been found experimentally, and the theoretical structures can be replaced by simple half integer or integer strength disclinations as shown, for example, in Figure 5.

Kleman[14] states that the cores of the τ disclinations are singular. But only in those cases where uneven numbers of π-turns are inserted into a cholesteric structure, is it necessary to envision half integer strength disclinations with singular cores. Similar considerations also apply in the case of "fingerprint textures".[30]

References

1. F. C. Frank, *Discuss. Faraday Soc.*, **25**, 19 (1958).
2. J. Nehring, *Phys. Rev.*, **A7**, 1737 (1973).
3. T. J. Scheffer, *Phys. Rev.*, **A5**, 1327 (1972).
4. M. Kleman, in *Advances in Liquid Crystals I*, Edited by G. H. Brown, Academic Press (1975).
5. P. G. de Gennes, *The Physics of Liquid Crystals*, Chapter 4, Clarendon Press, Oxford (1974).
6. J. Friedel and P. G. de Gennes, *C.R.Acad. Sci. Paris*, **268**, 257 (1969).
7. P. E. Cladis and M. Kleman, *J. Phys. (Paris)*, **33**, 591 (1972).
8. R. B. Meyer, *Phil. Mag.*, **27**, 405 (1973).
9. J. Nehring and A. Saupe, *J. Chem. Soc.*, Faraday Trans. II 68, 1 (1972).
10. M. Kleman and J. Friedel, *J. Phys. (Paris)*, **30**, C4-43 (1969).
11. R. Cano, *Bull. Soc. Miner. Crist.*, **90**, 333 (1967).
12. P. G. de Gennes, *The Physics of Liquid Crystals*, Chapter 6, Clarendon Press. Oxford (1974).
13. Y. Bouligand and M. Kleman, *J. Phys. (Paris)*, **31**, 1041 (1970).
14. M. Kleman, in *Liquid Crystals and Plastic Crystals I*, Chapter 3. Edited by G. W. Gray and P. A. Winsor, John Wiley and Sons, New York (1974).
15. A. Saupe, *Mol. Cryst. Liq. Cryst.*, **21**, 211 (1973).
16. J. Rault, Thesis, Orsay (1971).
17. A. Stieb, Thesis, Freiburg (1975).

18. C. J. Gerritsma, J. J. M. J. de Klerk, and P. v. Zanten, *Solid State Commun.*, **17**, 1077 (1975).
19. G. Baur, A. Stieb, and G. Meier, *Appl. Phys.*, **2**, 349 (1973).
20. R. Steinstraesser, *Angew. Chemie*, **84**, 636 (1972).
21. W. H. De Jeu, C. J. Gerritsma, P. v. Zanten, and W. J. A. Goossens, *Phys. Lett.*, **39A**, 355 (1972).
22. W. Helfrich, *Phys. Rev. Lett.*, **21**, 1518 (1968).
23. A. Stieb, G. Baur, and G. Meier, *J. Phys.* (*Paris*), **36**, C1-185, (1975).
24. C. Z. v. Doorn, *J. Phys.* (*Paris*), **36**, C1-261 (1975)
25. M. Schadt and W. Helfrich, *Appl. Phys. Lett.*, **18**, 127 (1971).
26. Groupe d'Orsay, *J. Phys.* (*Paris*), **30**, C4-38 (1969).
27. V. Vitek, M. Kleman, *J. Phys.* (*Paris*), **36**, 59 (1975).
28. J. L. Ericksen, in *Liquid Crystals and Orderd Fluids I*, p. 181, Edited by J. F. Johnson and R. S. Porter, Plenum Press, New York (1970).
29. F. R. N. Nabarro, *J. Phys.* (*Paris*), **33**, 1089 (1972).
30. P. E. Cladis, M. Kleman, *Mol. Cryst. Liq. Cryst.*, **16**, 1 (1972).